Pseudo-clock biases for precise point positioning. The algebraic approach

A. Lannes[1] S. Gratton[2] S. Durand[3]

[1]CNRS/Supelec/Univ Paris-Sud (France)
[2]UPS/INPT-IRIT/Enseeiht (France)
[3]ESGT/CNAM (France)

Abstract

As shown in a companion paper devoted to GNSS networks in algebraic graph theory, any (real- or) integer-valued function taking its values on the edges of the GNSS graph can be regarded as the sum of three (real- or) integer-valued functions: a function taking its values on the receiver vertices of this graph, another one on the satellite vertices, and the last one, the closure-delay (CD) function, taking its values on the loop-closure edges. For a given spanning tree, this decomposition is unique. The notion of closure delay generalizes that of double difference (DD). In this framework, particular satellite biases can be estimated and broadcasted to the network users for their precise point positioning (PPP). For example, in the case of large networks, each of these biases includes three (or four) terms: a satellite-clock term, a satellite time-group term, a satellite ionospheric term, and (for the phase) a satellite integer ambiguity multiplied by the corresponding wavelength. The form of the PPP equations to be solved by the network user is then the same as that of the traditional PPP equations. As soon as the CD ambiguities are fixed and validated, estimates of these float biases can be obtained. The main result of this paper is that no other ambiguity is then to be fixed, hence a better efficiency. In particular, in this approach, it is not necessary to fix the carrier-phase ambiguities, a problem which cannot be easily solved. Indeed, as shown in this paper, when the CD ambiguities are fixed (or when a maximum set of DD ambiguities is fixed), the remaining float problem is not of full rank.

Keywords. GNSS networks. Clock biases. RTK. PPP.

1. Introduction

The global positioning techniques are based on the following observational equations. For each frequency ν, for each receiver-satellite pair $(i, j) \equiv (r_i, s_j)$, and at each epoch t, the carrier-phase and code data are respectively of the form (see, e.g., Teunissen and Kleusberg 1998)

$$
\begin{aligned}
\Phi_{\nu,t}(i,j) = {} & \rho_t(i,j) + T_t(i,j) - \kappa_\nu I_t(i,j) \\
& + [f_{\phi;t}^{(r)}(i) - f_{\phi;t}^{(s)}(j)] - \kappa_\nu [g_{\phi;t}^{(r)}(i) - g_{\phi;t}^{(s)}(j)] \\
& + \lambda_\nu N_\nu(i,j) + \varepsilon_{\phi;\nu,t}(i,j)
\end{aligned} \tag{1}
$$

$$
\begin{aligned}
P_{\nu,t}(i,j) = {} & \rho_t(i,j) + T_t(i,j) + \kappa_\nu I_t(i,j) \\
& + [f_{p;t}^{(r)}(i) - f_{p;t}^{(s)}(j)] + \kappa_\nu [g_{p;t}^{(r)}(i) - g_{p;t}^{(s)}(j)] \\
& + \varepsilon_{p;\nu,t}(i,j)
\end{aligned} \tag{2}
$$

In these equations, which are expressed in length units, $\rho_t(i,j)$ is the receiver-satellite range: the distance between satellite s_j (at the time $t - \tau$ where the signal is emitted) and receiver r_i (at the time t of its reception); $T_t(i,j)$ and $I_t(i,j)$ are the tropospheric and ionospheric delays, respectively. Here,

$$
\kappa_\nu = \nu_1^2/\nu^2 = \lambda_\nu^2/\lambda_1^2 \tag{3}
$$

The λ_ν's denote the wavelengths of the carrier waves involved in the observational process. Note that $\kappa_{\nu_1} = 1$. The integers $N_\nu(i,j)$ are the integer carrier-phase ambiguities: $N_\nu(i,j) \in \mathbb{Z}$.

The instrumental biases and the clock errors depending only on r_i and t are lumped together in the 'extended receiver-clock biases' $f_{\phi;t}^{(r)}(i)$, $f_{p;t}^{(r)}(i)$. Likewise, the instrumental biases and the clock errors depending only on s_j and t are lumped together in the 'extended satellite-clock biases' $f_{\phi;t}^{(s)}(j)$, $f_{p;t}^{(s)}(j)$. Similarly, $g_{\phi;t}^{(r)}(i)$, $g_{p;t}^{(r)}(i)$ and $g_{\phi;t}^{(s)}(j)$, $g_{p;t}^{(s)}(j)$ denote the biases involved in the definition of the time-group delays.

In this model, the expectation values of the noise terms $\varepsilon_{\phi;\nu,t}(i,j)$ and $\varepsilon_{p;\nu,t}(i,j)$ are supposed to be zero. We also assume that these noises are not mutually correlated.

Lannes et al: Pseudo-clock biases for precise point positioning. The algebraic approach

69

In this paper, we consider a GNSS network and particular satellite biases. Estimates of these pseudo-clock biases are broadcasted to the network users for their precise point positioning (PPP). The theoretical framework is presented in Sect. 2. Once the linearization aspects have been specified (Sect. 3), the corresponding approach is then introduced (Sect. 4). The similarities and differences with other related approaches are examined in that framework. Section 5 is devoted to the optimization technique that provides the pseudo-clock biases in question. Some comments on the key points of our contribution are to be found in Sect. 6.

2. Theoretical Framework

Let us consider a GNSS network including m stations, and thereby m multifrequency receivers r_i. The number of satellites s_j involved in the observational process over some time interval $[t_1, \ t_\ell]$ is denoted by n. The 'observational grid' of the network is therefore a grid G_o including m lines, n columns, and mn points; see Fig. 1. For example, in the case of large networks, m and n are of the order of 100 and 32, respectively. A function such as Φ_{ν,t_k} or ρ_{t_k}, with k in $[1, \ \ell]$, takes its values on some points (i,j) of G_o. These points form a subset of G_o denoted by G_k: the 'GNSS grid' of epoch t_k. When no confusion may arise, subscript k is omitted: $G \equiv G_k$. The ith line of G is denoted by $\mathcal{L}_i$:

$$\mathcal{L}_i := \{j : (i,j) \in G, \ i \text{ being fixed}\} \tag{4}$$

Likewise, the set

$$\mathcal{C}_j := \{i : (i,j) \in G, \ j \text{ being fixed}\} \tag{5}$$

characterizes the jth column of G.

2.1. GNSS graph. Edge-delay space

In the example presented in the upper part of Fig. 1, the points (i,j) of G are shown as black dots. As illustrated in the lower part of this figure, these points correspond to the 'edges' (r_i, s_j) of the GNSS graph to be considered; $\mathcal{E}$ denotes the set of its edges; n_e is their number. The receivers and the satellites involved in the definition of these edges define the 'vertices' of this graph; $\mathcal{V}$ denotes the set of its vertices, and n_v their number:

$$n_v = m + n \tag{6}$$

A GNSS graph $\mathcal{G}$ is therefore defined by the pair $(\mathcal{V}, \mathcal{E})$: $\mathcal{G} \equiv \mathcal{G}(\mathcal{V}, \mathcal{E})$. For simplicity, we now assume that $\mathcal{G}$ is connected (e.g., Biggs 1996): given any two vertices of $\mathcal{V}$, there exists a path of edges of $\mathcal{E}$ connecting these vertices. (If this is not the case, $\mathcal{G}$ is reduced to its main connected component; G is then reduced consequently.)

A function ϑ taking its values on G, and thereby on $\mathcal{E}$, can be regarded as a vector of $E := \mathbb{R}^{n_e}$. The values of ϑ on G are then regarded as the components of ϑ in the standard basis of this edge-delay space.
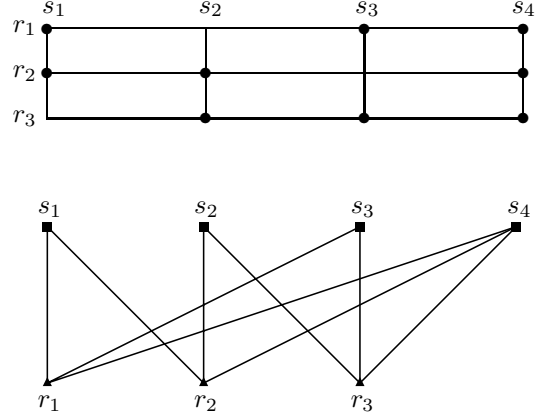

Figure 1: *GNSS grid G and GNSS graph* $\mathcal{G}$. In the example shown here, the observational grid G_o includes 12 points: $m = 3$, $n = 4$. The GNSS grid of epoch t_k, $G \equiv G_k$, includes 9 points; these points are shown as black dots. The corresponding graph, $\mathcal{G} \equiv \mathcal{G}_k$, includes 7 vertices and 9 edges: $n_v = m + n = 7$, $n_e = 9$. The data corresponding to the receiver-satellite pairs (r_1, s_2), (r_2, s_3) and (r_3, s_1) are missing.

2.2. GNSS spanning tree and loops

As illustrated in Fig. 2, a spanning tree of $\mathcal{G} \equiv \mathcal{G}(\mathcal{V}, \mathcal{E})$ is a subgraph $\mathcal{G}_{st} \equiv \mathcal{G}(\mathcal{V}, \mathcal{E}_{st})$ formed by n_v vertices and $n_v - 1$ edges, with no 'cycle' in it. Here, 'cycle' is used in the sense defined in algebraic graph theory (Biggs 1996). In the GNSS community, to avoid any confusion with the usual notion of wave cycle, it is not forbidden to substitute the term of 'loop' for that of 'cycle.' In this context, the number of loops defined through a given fixed (but arbitrary) spanning tree is the number of edges of $\mathcal{E}$ that do not lie in $\mathcal{E}_{st}$. These edges,

$$c(q) := (r_{i(q)}, s_{j(q)}) \tag{7}$$

are said to be 'loop-closure edges' (see Fig. 2). Their number is denoted by n_c:

$$n_c = n_e - (n_v - 1) \qquad (n_v = m + n, \ n_e \leq mn) \tag{8}$$

To select a GNSS spanning tree, the edges of $\mathcal{E}$ are first ordered somehow. The corresponding sequence is of the form

$$e(q) := (r_{i_q}, s_{j_q}) \qquad (q = 1, \ldots, n_e)$$

The algorithm is the following: set $q = 0$, $n_{st} = 0$, and $\mathcal{E}_{st} = \emptyset$ (the empty set). Then,

(1) If $n_{st} = n_v - 1$, terminate the process; otherwise, set $q \overset{\text{set}}{=} q + 1$.

(2) When the vertices of $e(q)$ are not connected via edges of $\mathcal{E}_{st}$, set $\mathcal{E}_{st} \overset{\text{set}}{=} \mathcal{E}_{st} \cup \{e(q)\}$ and $n_{st} \overset{\text{set}}{=} n_{st} + 1$; then go to step (1).

Lannes et al: Pseudo-clock biases for precise point positioning. The algebraic approach
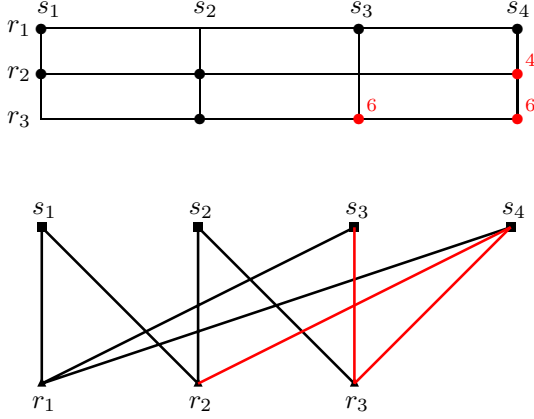
70

Figure 2: *GNSS spanning tree and loops.* The black edges of $\mathcal{G}$ (the graph introduced in Fig. 1) are the edges of the selected spanning tree $\mathcal{G}_{\mathrm{st}}$. The points of the corresponding subgrid G_{st} are shown as black dots. The remaining points of G (the red dots of G) correspond to the loop-closure edges (the red edges of $\mathcal{G}$). We then have one loop of order 4, and 2 loops of order 6: (r_2 , s_4 , r_1 , s_1), $(r_3, s_3, r_1, s_1, r_2, s_2)$ and $(r_3, s_4, r_1, s_1, r_2, s_2)$. These orders are shown as red numbers.

The subgrid of G corresponding to the edges of $\mathcal{E}_{\mathrm{st}}$ is denoted by G_{st}. By construction, the spanning tree thus found depends on how the edges are ordered.

Example 2.1. To show, in concrete manner, how this algorithm works, we now consider its action on the grid G of Fig. 2, its points being ordered line by line.

The points of the first line of G, the points $(1, 1)$, $(1, 3)$ and $(1, 4)$, define the first 3 edges of $\mathcal{E}_{\mathrm{st}}$:

$$\mathcal{E}_{\mathrm{st}} \stackrel{\mathrm{set}}{=} \{(r_1, s_1), (r_1, s_3), (r_1, s_4)\} \qquad (n_{\mathrm{st}} = 3)$$

By construction, four vertices of $\mathcal{G}$ are then connected: r_1, s_1, s_3 and s_4.

The next point of G, the first point of line 2, is associated with edge (r_2, s_1). As r_2 and s_1 are not connected via edges of $\mathcal{E}_{\mathrm{st}}$, this edge cannot be a loop-closure edge. We therefore set

$$\mathcal{E}_{\mathrm{st}} \stackrel{\mathrm{set}}{=} \mathcal{E}_{\mathrm{st}} \cup \{(r_2, s_1)\} \qquad (n_{\mathrm{st}} = 4)$$

Five vertices are then connected: r_1, s_1, s_3, s_4 and r_2.

The next point of line 2 is associated with edge (r_2, s_2). As r_2 and s_2 are not connected via edges of $\mathcal{E}_{\mathrm{st}}$, we set

$$\mathcal{E}_{\mathrm{st}} \stackrel{\mathrm{set}}{=} \mathcal{E}_{\mathrm{st}} \cup \{(r_2, s_2)\} \qquad (n_{\mathrm{st}} = 5)$$

Six vertices are then connected: r_1, s_1, s_3, s_4, r_2 and s_2.

The next point of G, the last point of line 2, is associated with edge (r_2, s_4). As r_2 and s_4 are already connected, this edge closes a loop with some edges of $\mathcal{E}_{\mathrm{st}}$. As a result, this edge is the first loop-closure edge: $\mathrm{c}(1) = (r_2, s_4)$; see Eq. (7). The corresponding loop, (r_2 , s_4 , r_1 , s_1), is of order 4: it includes 4 edges (see Fig. 2).

The next point of G, the second point of line 3, is associated with edge (r_3, s_2). As r_3 and s_2 are not connected via edges of $\mathcal{E}_{\mathrm{st}}$, we then set

$$\mathcal{E}_{\mathrm{st}} \stackrel{\mathrm{set}}{=} \mathcal{E}_{\mathrm{st}} \cup \{(r_3, s_2)\} \qquad (n_{\mathrm{st}} = 6)$$

As all the vertices of $\mathcal{E}$ are then connected, the algorithm stops: $\mathcal{E}_{\mathrm{st}}$ is then completely defined.

The remaining points of line 3 therefore define two loop-closure edges: $\mathrm{c}(2) = (r_3, s_3)$ and $\mathrm{c}(3) = (r_3, s_4)$. These loops are of order 6; see Fig. 2.

Remark 2.1. In the special case of the graph shown in Fig. 2, there exist particular spanning trees for which the three loops are of order 4. As the choice of the spanning tree is arbitrary, it is not useful to search for such spanning trees.

Remark 2.2. In Example 2.1, the points of G are ordered line by line. In fact, to handle some graph transitions (i.e., some scenario changes), one may be led to order them in a more subtle manner; see Sect. 7.4.3 in Lannes and Gratton 2009.

2.3. Reference properties

The properties presented in this section are established in Sect. 4.2 of Lannes and Gratton 2009. We first introduce the notion of 'bias-delay space.'

Bias-delay space. The subspace of E whose functions β are of the form

$$\beta(i, j) = \delta^{[\mathrm{r}]}(i) + \delta^{[\mathrm{s}]}(j) \quad \text{with} \quad \delta^{[\mathrm{s}]}(1) = 0 \qquad (9)$$

is denoted by F. This subspace can be referred to as the bias-delay space. By definition, the 'receiver-delay space' $F^{[\mathrm{r}]}$ is the subspace of F whose functions β depend only on i: $\beta(i, j) = \delta^{[\mathrm{r}]}(i)$. Similarly, the 'satellite-delay space' $F^{[\mathrm{s}]}$ is the subspace of F whose functions are of the form $\beta(i, j) = \delta^{[\mathrm{s}]}(j)$ with $\delta^{[\mathrm{s}]}(1) = 0$. By construction, F is the 'oblique direct sum' of $F^{[\mathrm{r}]}$ and $F^{[\mathrm{s}]}$:

$$F = F^{[\mathrm{r}]} + F^{[\mathrm{s}]} \qquad F^{[\mathrm{r}]} \cap F^{[\mathrm{s}]} = \{0\}$$

We thus have

$$\dim F^{[\mathrm{r}]} = m \qquad \dim F^{[\mathrm{s}]} = n - 1 \qquad (10)$$

$$\dim F = \dim F^{[\mathrm{r}]} + \dim F^{[\mathrm{s}]} = n_{\mathrm{v}} - 1 \qquad (11)$$

Property 1. *Given any edge-delay function ϑ taking its values on G, for each spanning tree $\mathcal{G}_{\mathrm{st}}$ of $\mathcal{G}$, there exists a unique set of receiver and satellite delays*

$$\left\{\vartheta^{[\mathrm{r}]}(i)\right\}_{i=1}^{m} \cup \left\{\vartheta^{[\mathrm{s}]}(j)\right\}_{j=1}^{n} \quad \text{with} \quad \vartheta^{[\mathrm{s}]}(1) = 0$$

such that $\vartheta(i, j) = \vartheta^{[\mathrm{r}]}(i) + \vartheta^{[\mathrm{s}]}(j)$ on the points of G_{st}.

More concretely, the following process provides these delays in a recursive manner; for further details, see Lannes and Gratton 2009.

Lannes et al: Pseudo-clock biases for precise point positioning. The algebraic approach

71

Recursive differential process. Set $\vartheta^{[\mathrm{s}]}(1) = 0$; then, span the points of G_{st} line by line (see Fig. 2 or Fig. 3). For each point (i,j) thus encountered, then proceed as follows.

If $\vartheta^{[\mathrm{s}]}(j)$ has already been fixed, and $\vartheta^{[\mathrm{r}]}(i)$ is not fixed yet, set

$$\vartheta^{[\mathrm{r}]}(i) = \vartheta(i,j) - \vartheta^{[\mathrm{s}]}(j)$$

If $\vartheta^{[\mathrm{r}]}(i)$ has already been fixed, and $\vartheta^{[\mathrm{s}]}(j)$ is not fixed yet, set

$$\vartheta^{[\mathrm{s}]}(j) = \vartheta(i,j) - \vartheta^{[\mathrm{r}]}(i)$$

To obtain all these delays, G_{st} is to be spanned in this way as many times as required. It is important to point out that the only operations involved in this process are differences. As a result, if ϑ is an integer-valued function, the receiver and satellite delays $\vartheta^{[\mathrm{r}]}(i)$ and $\vartheta^{[\mathrm{s}]}(j)$ lie in $\mathbb{Z}$.

Example 2.2. To illustrate this recursive differential process, we now follow its action on the grid G_{st} of Fig. 2. As $\vartheta^{[\mathrm{s}]}(1)$ is nought, we then obtain successively:

$$\vartheta^{[\mathrm{r}]}(1) = \vartheta(1,1) - \vartheta^{[\mathrm{s}]}(1) = \vartheta(1,1)$$
$$\vartheta^{[\mathrm{s}]}(3) = \vartheta(1,3) - \vartheta^{[\mathrm{r}]}(1)$$
$$\vartheta^{[\mathrm{s}]}(4) = \vartheta(1,4) - \vartheta^{[\mathrm{r}]}(1)$$
$$\vartheta^{[\mathrm{r}]}(2) = \vartheta(2,1) - \vartheta^{[\mathrm{s}]}(1) = \vartheta(2,1)$$
$$\vartheta^{[\mathrm{s}]}(2) = \vartheta(2,2) - \vartheta^{[\mathrm{r}]}(2)$$
$$\vartheta^{[\mathrm{r}]}(3) = \vartheta(3,2) - \vartheta^{[\mathrm{s}]}(2)$$

Closure delays. According to Property 1, the quantities

$$\vartheta^{[\mathrm{cd}]}(i,j) := \vartheta(i,j) - \big[\vartheta^{[\mathrm{r}]}(i) + \vartheta^{[\mathrm{s}]}(j)\big] \qquad (12)$$

vanish on the points of G_{st}. The values of $\vartheta^{[\mathrm{cd}]}$ of interest are therefore defined on the remaining points of G, i.e., on the 'CD subgrid'

$$G_{\mathrm{cd}} := \{(i,j) \in G : (i,j) \notin G_{\mathrm{st}}\} \qquad (13)$$

Clearly, G_{cd} includes n_{c} loop-closure points; see Eq. (8) and Figs. 2 & 3. The quantities $\vartheta^{[\mathrm{cd}]}(i,j)$ on G_{cd} can therefore be referred to as the 'closure delays' of ϑ, hence the notation cd or CD.

The notion of closure delay generalizes that of double difference. In fact, for a given loop, the closure delay of ϑ is the 'alternate algebraic sum' of the values of ϑ along the edges of that loop. For example, with regard to Fig. 3, the CD ambiguity $N_\nu^{[\mathrm{cd}]}(3,3)$ is the alternate sum

$$N_\nu(3,3) - N_\nu(3,2) + N_\nu(2,2) - N_\nu(2,1) + N_\nu(1,1) - N_\nu(1,3)$$

As clarified in a paper to appear in the Journal of Geodesy (Lannes and Teunissen 2010/11), the CD ambiguities are the 'estimable functions of carrier-wave ambiguities' of de Jonge 1998. These functions were introduced to correct for rank defects of the undifferenced equations; see Teunissen 1984.
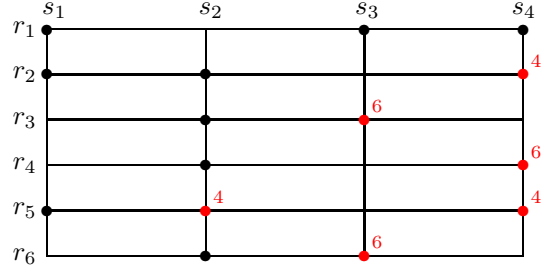

Figure 3: *Interest of the CD approach.* In the scenario considered here, G includes 15 points. The selected spanning tree is built by spanning the points of G line by line. The points of G_{st} are shown as black dots. The red ones are the corresponding loop-closure points; see Fig. 2. With regard to the selected spanning tree, we then have 3 loops of order 4, and 3 loops of order 6. Here, the 'maximum number of independent double differences' is equal to 5; for further details see Eq. (46). In the corresponding DD approach, the data of grid point $(1,3)$ are not used; see Fig. 4. The CD approach is therefore preferable since all the data are then processed.

Property 2. *Any edge-delay function ϑ taking its values on G can be decomposed in the form*

$$\vartheta(i,j) = \vartheta^{[\mathrm{r}]}(i) + \vartheta^{[\mathrm{s}]}(j) + \vartheta^{[\mathrm{cd}]}(i,j)$$

For a given spanning tree, this decomposition is unique.

This property is a simple transcription of Eq. (12). The uniqueness of this decomposition results from Property 1.

Example 2.3. With regard to the GNSS grid of Fig. 2, let us consider (for simplicity) the ambiguity function

$$N: \begin{bmatrix} 2 & * & 1 & -1 \\ -1 & 1 & * & 1 \\ * & -2 & 2 & -1 \end{bmatrix}$$

The recursive differential process of Example 2.2 applied to this function yields the following components:

$$N^{[\mathrm{r}]}: \begin{bmatrix} 2 & * & 2 & 2 \\ -1 & -1 & * & -1 \\ * & -4 & -4 & -4 \end{bmatrix}$$

$$N^{[\mathrm{s}]}: \begin{bmatrix} 0 & * & -1 & -3 \\ 0 & 2 & * & -3 \\ * & 2 & -1 & -3 \end{bmatrix}$$

$$N^{[\mathrm{cd}]}: \begin{bmatrix} 0 & * & 0 & 0 \\ 0 & 0 & * & 5 \\ * & 0 & 7 & 6 \end{bmatrix}$$

Lannes et al: Pseudo-clock biases for precise point positioning. The algebraic approach

72

Remark 2.3. To handle some graph transitions, one may be led to change the selected spanning tree (see Remark 2.2). The CD ambiguity variables are then transformed accordingly. The corresponding linear operators can easily be determined.

Remark 2.4. It can be shown that the maximum number of independent double differences is less than or equal to n_{c}; see Lannes and Teunissen 2010/11. An example where this number is strictly less than n_{c} is given in Fig. 3.

3. Linearization

For clarity, let us now substitute k for t_k. In most cases encountered in practice, the functional variable ρ_k can be linearly expanded in terms of other variables. In the general case, some of the latter depend on k, while others not; see, e.g., Feng and Li 2008. In other terms, the first ones are 'local' variables, while the others are 'global' with however possible transitions from time to time.

More precisely, the receiver-satellite range can be expanded in the form

$$\rho_k(i,j) = \rho_k^0(i,j) + \sum_{\mathsf{p}=1}^3 c_{k;\mathsf{p}}(i,j)\, u_{i,k;\mathsf{p}}^{(\xi)} \tag{14}$$
$$+ \sum_{\mathsf{q}} d_{k;\mathsf{q}}(i,j)\, v_{\mathsf{q}}$$

Here, $\rho_k^0(i,j)$ is the nominal value of $\rho_k(i,j)$; $u_{i,k;\mathsf{p}}^{(\xi)}$ is the pth increment variable of (the position of) receiver r_i at epoch k. Note that $c_{k;\mathsf{p}}(i,j)$ is a direction-cosine function; see, e.g., Eq. (14) in Lannes and Gratton 2008. The $u_{i,k;\mathsf{p}}^{(\xi)}$'s are the position components of the local variable u_k. When the positions of some receivers are expanded as 'piecewise polynomial functions' of t, the parameters involved in these expansions appear in the definition of the global variables v_{q}; and likewise when orbital parameters are to be refined. Clearly, the v_{q}'s are components of some global variable v. The functions $d_{k;\mathsf{q}}(i,j)$ characterize the corresponding global expansion term at epoch k.

Similarly, in most cases encountered in practice, one may refer to a tropospheric model of the form

$$T_k(i,j) = b_k(i,j)\, u_{i,k}^{(\tau)} \tag{15}$$

where $u_{i,k}^{(\tau)}$ is the zenith tropospheric variable of receiver r_i at epoch k; for further details on this point, see Ge *et al* 2006. The $u_{i,k;\mathsf{p}}^{(\tau)}$'s are the tropospheric components of the local variable u_k. Like $c_{k;\mathsf{p}}(i,j)$, $b_k(i,j)$ is a known function which takes into account the receiver-satellite geometry.

For simplicitly, we now restrict ourselves to the case of large networks. In that case, the functions b_k and $c_{k;\mathsf{p}}$ effectively depend on i and j.

4. The Algebraic Approach: Survey

We first introduce the reference equations of our approach: Sect. 4.1. We then give a survey of the methods to be implemented for solving the problem: Sect. 4.2. The related PPP equations are specified in Sect. 4.3. We finally make some comments on the similarities and the differences with other related approaches: Sect. 4.4.

4.1. Reference equations

For $\mu = \phi$ or p, let us set

$$\left|\begin{aligned} \delta_{\mu;\nu,k}^{[\mathrm{r}]}(i) &:= \delta_{\mu;\nu,k}^{(\mathrm{r})}(i) + \delta_{\mu;\nu,k}^{(\mathrm{s})}(1) \\ \delta_{\mu;\nu,k}^{[\mathrm{s}]}(j) &:= \delta_{\mu;\nu,k}^{(\mathrm{s})}(j) - \delta_{\mu;\nu,k}^{(\mathrm{s})}(1) \end{aligned}\right. \tag{16}$$

in which

$$\left|\begin{aligned} \delta_{\phi;\nu,k}^{(\mathrm{r})}(i) &:= [f_{\phi;k}^{(\mathrm{r})}(i) - \kappa_\nu g_{\phi;k}^{(\mathrm{r})}(i)] \\ \delta_{\phi;\nu,k}^{(\mathrm{s})}(j) &:= -[f_{\phi;k}^{(\mathrm{s})}(j) - \kappa_\nu g_{\phi;k}^{(\mathrm{s})}(j)] \end{aligned}\right. \tag{17}$$

and

$$\left|\begin{aligned} \delta_{p;\nu,k}^{(\mathrm{r})}(i) &:= [f_{p;k}^{(\mathrm{r})}(i) + \kappa_\nu g_{p;k}^{(\mathrm{r})}(i)] \\ \delta_{p;\nu,k}^{(\mathrm{s})}(j) &:= -[f_{p;k}^{(\mathrm{s})}(j) + \kappa_\nu g_{p;k}^{(\mathrm{s})}(j)] \end{aligned}\right. \tag{18}$$

By construction (see Eq. (16)), we have $\delta_{\mu;\nu,k}^{[\mathrm{s}]}(1) = 0$.

The linearized observational equations can then be written in the forms (see Eqs. (1), (2), (14) and (15))

$$\Phi_{\nu,k}^0(i,j) = \sum_{\mathsf{p}=1}^3 c_{k;\mathsf{p}}(i,j)\, u_{i,k;\mathsf{p}}^{(\xi)} + \sum_{\mathsf{q}} d_{k;\mathsf{q}}(i,j)\, v_{\mathsf{q}}$$
$$+ b_k(i,j)\, u_{i,k}^{(\tau)} - \kappa_\nu I_k(i,j)$$
$$+ [\delta_{\phi;\nu,k}^{[\mathrm{r}]}(i) + \delta_{\mu;\nu,k}^{[\mathrm{s}]}(j)] \tag{19}$$
$$+ \lambda_\nu N_\nu(i,j) + \varepsilon_{\phi;\nu,k}(i,j)$$

$$P_{\nu,k}^0(i,j) = \sum_{\mathsf{p}=1}^3 c_{k;\mathsf{p}}(i,j)\, u_{i,k;\mathsf{p}}^{(\xi)} + \sum_{\mathsf{q}} d_{k;\mathsf{q}}(i,j)\, v_{\mathsf{q}}$$
$$+ b_k(i,j)\, u_{i,k}^{(\tau)} + \kappa_\nu I_k(i,j) \tag{20}$$
$$+ [\delta_{p;\nu,k}^{[\mathrm{r}]}(i) + \delta_{p;\nu,k}^{[\mathrm{s}]}(j)] + \varepsilon_{p;\nu,k}(i,j)$$

where

$$\Phi_{\nu,k}^0(i,j) := \Phi_{\nu,k}(i,j) - \rho_k^0(i,j) \tag{21}$$

$$P_{\nu,k}^0(i,j) := P_{\nu,k}(i,j) - \rho_k^0(i,j) \tag{22}$$

The algebraic approach presented in this paper is based on Property 2. With regard to the selected spanning tree, the carrier-phase ambiguity functions are then decomposed in the form

$$N_\nu(i,j) = N_\nu^{[\mathrm{r}]}(i) + N_\nu^{[\mathrm{s}]}(j) + N_\nu^{[\mathrm{cd}]}(i,j) \quad \text{(on } G\text{)} \tag{23}$$

We are then led to introduce the quantities

$$\left|\begin{aligned} \bar{\delta}_{\phi;\nu,k}^{[\mathrm{r}]}(i) &:= \delta_{\phi;\nu,k}^{[\mathrm{r}]}(i) + \lambda_\nu N_\nu^{[\mathrm{r}]}(i) \\ \bar{\delta}_{\phi;\nu,k}^{[\mathrm{s}]}(j) &:= \delta_{\phi;\nu,k}^{[\mathrm{s}]}(j) + \lambda_\nu N_\nu^{[\mathrm{s}]}(j) \end{aligned}\right. \tag{24}$$

As $N_\nu^{[\mathrm{s}]}(1) = 0$, we have $\bar{\delta}_{\phi;\nu,k}^{[\mathrm{s}]}(1) = 0$.

Lannes et al: Pseudo-clock biases for precise point positioning. The algebraic approach

73

In the absence of reliable ionospheric model, the ionospheric delays are also decomposed:

$$I_k(i,j) = I_k^{[\text{r}]}(i) + I_k^{[\text{s}]}(j) + I_k^{[\text{cd}]}(i,j) \qquad \text{(on } G\text{)} \quad (25)$$

The clock biases to be considered are then of the form

$$\left|\begin{array}{rcl} \tilde{\delta}_{\phi;\nu,k}^{[\text{r}]}(i) & := & \bar{\delta}_{\phi;\nu,k}^{[\text{r}]}(i) - \kappa_\nu I_k^{[\text{r}]}(i) \\[2mm] \tilde{\delta}_{\phi;\nu,k}^{[\text{s}]}(j) & := & \bar{\delta}_{\phi;\nu,k}^{[\text{s}]}(j) - \kappa_\nu I_k^{[\text{s}]}(j) \end{array}\right. \quad (26)$$

and

$$\left|\begin{array}{rcl} \tilde{\delta}_{p;\nu,k}^{[\text{r}]}(i) & := & \delta_{p;\nu,k}^{[\text{r}]}(i) + \kappa_\nu I_k^{[\text{r}]}(i) \\[2mm] \tilde{\delta}_{p;\nu,k}^{[\text{s}]}(j) & := & \delta_{p;\nu,k}^{[\text{s}]}(j) + \kappa_\nu I_k^{[\text{s}]}(j) \end{array}\right. \quad (27)$$

Again, as $I_k^{[\text{s}]}(1) = 0$, we have $\tilde{\delta}_{\mu;\nu,k}^{[\text{s}]}(1) = 0$. The phase and code equations to be considered can then be written in the respective forms

$$\Phi_{\nu,k}^0(i,j) = \sum_{\mathsf{p}=1}^3 c_{k;\mathsf{p}}(i,j)\, u_{i,k;\mathsf{p}}^{(\xi)} + \sum_{\mathsf{q}} d_{k;\mathsf{q}}(i,j)\, v_{\mathsf{q}}$$
$$+\, b_k(i,j)\, u_{i,k}^{(\tau)} - \kappa_\nu I_k^{[\text{cd}]}(i,j) \quad (28)$$
$$+\, \lambda_\nu N_\nu^{[\text{cd}]}(i,j) + \tilde{\beta}_{\phi;\nu,k}(i,j) + \varepsilon_{\phi;\nu,k}(i,j)$$

$$P_{\nu,k}^0(i,j) = \sum_{\mathsf{p}=1}^3 c_{k;\mathsf{p}}(i,j)\, u_{i,k;\mathsf{p}}^{(\xi)} + \sum_{\mathsf{q}} d_{k;\mathsf{q}}(i,j)\, v_{\mathsf{q}}$$
$$+\, b_k(i,j)\, u_{i,k}^{(\tau)} + \kappa_\nu I_k^{[\text{cd}]}(i,j) \quad (29)$$
$$+\, \tilde{\beta}_{p;\nu,k}(i,j) + \varepsilon_{p;\nu,k}(i,j)$$

where, for $\mu = \phi$ or p (see Eq. (9)),

$$\tilde{\beta}_{\mu;\nu,k}(i,j) := \tilde{\delta}_{\mu;\nu,k}^{[\text{r}]}(i) + \tilde{\delta}_{\mu;\nu,k}^{[\text{s}]}(j) \quad (30)$$

When three carrier waves are available, this approach is particularly recommended. Indeed, no ionospheric model is then introduced.

4.2. Solution of the problem

The analysis presented in Lannes and Gratton (2009) can be transposed to Eqs. (28) and (29). The local functional variables $\tilde{\beta}_{\phi;\nu,k}$ and $\tilde{\beta}_{p;\nu,k}$ are then regarded as particular variables of the problem. The other local variables $u_{i,k;\mathsf{p}}^{(\xi)}$, $u_{i,k}^{(\tau)}$ and $I_k^{[\text{cd}]}(i,j)$ on G_{cd} are lumped together in some variable u_k. The global variable v includes two main components. The first one, v_{b}, is that defined by the real variables v_{q}, whereas the second, v_{c}, is that defined by the values the integer CD ambiguities to be fixed. We thus have on G_{cd}: $v_{\text{c};\nu} \equiv N_\nu^{[\text{cd}]}$. Equations (28) and (29) are then written in the respective functional forms

$$\Phi_{\nu,k}^0 = \text{A}_{\phi;\nu,k} u_k + (\text{B}_k v_{\text{b}} + \lambda_\nu v_{\text{c};\nu}) + \tilde{\beta}_{\phi;\nu,k} + \varepsilon_{\phi;\nu,k} \quad (31)$$

$$P_{\nu,k}^0 = \text{A}_{p;\nu,k} u_k + \text{B}_k v_{\text{b}} + \tilde{\beta}_{p;\nu,k} + \varepsilon_{p;\nu,k} \quad (32)$$

where $\text{A}_{\phi;\nu,k}$, $\text{A}_{p;\nu,k}$ and B_k are linear operators.

As shown in Lannes and Gratton 2009, the corresponding float problem can be solved in the least-square sense, recursively, by using the QR method; see, e.g., Björck 1996. Other recursive least-square techniques can of course be implemented; see, e.g., de Jonge 1998. At each epoch, these methods provide the 'float ambiguity vector' $\hat{v}_{k;\text{c}}$ and the Cholesky factor $R_{k;\text{c}}$ of the inverse of its variance-covariance matrix. This upper-triangular matrix is then 'decorrelated.' In our approach, this is done on the grounds of the LLL algorithm; see, e.g., Sect. 8.2 in Lannes and Gratton 2009. Once $R_{k;\text{c}}$ has thus been decorrelated, the integer ambiguity solution $\check{v}_{k;\text{c}}$ is obtained by using classical integer-programming techniques. Once $\check{v}_{k;\text{c}}$ has been fixed to some $\check{v}_{\text{c}}$ (" $\check{v}_{k;\text{c}} \to \check{v}_{\text{c}}$"), and $\check{v}_{\text{c}}$ has been validated, the problem can be completely solved. Indeed, we then have $\check{v}_{\text{c}} \equiv N^{[\text{cd}]}$. The corresponding estimates of u_k and v_{b} are then denoted by $\check{u}_k$ and $\check{v}_{\text{b}}$, respectively.

In particular, as specified in Sect. 5, estimates of the satellite biases $\tilde{\delta}_{\mu;\nu,k}^{[\text{s}]}(j)$ for $j \neq 1$ are thus obtained. These estimates, denoted by $\check{\delta}_{\mu;\nu,k}^{[\text{s}]}(j)$, are referred to as the 'satellite pseudo-clock biases.' They can be broadcasted to the network users for their precise point positioning. As clarified in Sect. 4.3, the equations to be solved by the user have then the form of the traditional PPP equations.

4.3. Related PPP equations

Let us denote by r_ι the user receiver. The observational equations (19) and (20) can then be written in the respective forms

$$\Phi_{\nu,k}^0(\iota,j) = \sum_{\mathsf{p}=1}^3 c_{k;\mathsf{p}}(\iota,j)\, u_{\iota,k;\mathsf{p}}^{(\xi)} + \sum_{\mathsf{q}} d_{k;\mathsf{q}}(\iota,j)\, v_{\mathsf{q}}$$
$$+\, b_k(\iota,j)\, u_{\iota,k}^{(\tau)} - \kappa_\nu I_k(\iota,j)$$
$$+\, [\delta_{\phi;\nu,k}^{[\text{r}]}(\iota) + \delta_{\mu;\nu,k}^{[\text{s}]}(j)] \quad (33)$$
$$+\, \lambda_\nu N_\nu(\iota,j) + \varepsilon_{\phi;\nu,k}(\iota,j)$$

$$P_{\nu,k}^0(\iota,j) = \sum_{\mathsf{p}=1}^3 c_{k;\mathsf{p}}(\iota,j)\, u_{\iota,k;\mathsf{p}}^{(\xi)} + \sum_{\mathsf{q}} d_{k;\mathsf{q}}(\iota,j)\, v_{\mathsf{q}}$$
$$+\, b_k(\iota,j)\, u_{\iota,k}^{(\tau)} + \kappa_\nu I_k(\iota,j) \quad (34)$$
$$+\, [\delta_{p;\nu,k}^{[\text{r}]}(\iota) + \delta_{p;\nu,k}^{[\text{s}]}(j)] + \varepsilon_{p;\nu,k}(\iota,j)$$

From Eqs. (24), (26) and (27), we have (with regard to the selected spanning tree of the GNSS network graph)

$$\left|\begin{array}{l} \delta_{\phi;\nu,k}^{[\text{s}]}(j) \simeq \check{\delta}_{\phi;\nu,k}^{[\text{s}]}(j) + \kappa_\nu I_k^{[\text{s}]}(j) - \lambda_\nu N_\nu^{[\text{s}]}(j) \\[2mm] \delta_{p;\nu,k}^{[\text{s}]}(j) \simeq \check{\delta}_{p;\nu,k}^{[\text{s}]}(j) - \kappa_\nu I_k^{[\text{s}]}(j) \end{array}\right. \quad (35)$$

We are then led to set

$$\left|\begin{array}{l} \Phi_{\nu,k}^{(\iota)}(j) := \Phi_{\nu,k}^0(\iota,j) - \check{\delta}_{\phi;\nu,k}^{[\text{s}]}(j) \\[2mm] P_{\nu,k}^{(\iota)}(j) := P_{\nu,k}^0(\iota,j) - \check{\delta}_{p;\nu,k}^{[\text{s}]}(j) \end{array}\right. \quad (36)$$

$$I_k^{(\iota)} := I_k(\iota,j) - I_k^{[\text{s}]}(j) \quad (37)$$

$$N_\nu^{(\iota)}(j) := N_\nu(\iota,j) - N_\nu^{[\text{s}]}(j) \quad (38)$$

Lannes et al: Pseudo-clock biases for precise point positioning. The algebraic approach

74

Equations (33) and (34) then yield the PPP equations

$$\Phi_{\nu,k}^{(\iota)}(j) = \sum_{\mathfrak{p}=1}^{3} c_{k;\mathfrak{p}}(\iota, j)\, u_{\iota,k;\mathfrak{p}}^{(\xi)} + \sum_{\mathfrak{q}} d_{k;\mathfrak{q}}(\iota, j)\, v_{\mathfrak{q}}$$
$$+ b_k(\iota, j)\, u_{\iota,k}^{(\tau)} - \kappa_\nu I_k^{(\iota)}(j) \quad (39)$$
$$+ \lambda_\nu N_\nu^{(\iota)}(j) + \delta_{\phi;\nu,k}^{[\mathrm{r}]}(\iota) + \tilde{\varepsilon}_{\phi;\nu,k}(\iota, j)$$

$$P_{\nu,k}^{(\iota)}(j) = \sum_{\mathfrak{p}=1}^{3} c_{k;\mathfrak{p}}(\iota, j)\, u_{\iota,k;\mathfrak{p}}^{(\xi)} + \sum_{\mathfrak{q}} d_{k;\mathfrak{q}}(\iota, j)\, v_{\mathfrak{q}}$$
$$+ b_k(\iota, j)\, u_{\iota,k}^{(\tau)} + \kappa_\nu I_k^{(\iota)}(j) \quad (40)$$
$$+ \delta_{p;\nu,k}^{[\mathrm{r}]}(\iota) + \tilde{\varepsilon}_{p;\nu,k}(\iota, j)$$

Clearly, as $\check{\delta}_{\mu;\nu,k}^{[\mathrm{s}]}$ is an estimate of $\check{\delta}_{\mu;\nu,k}^{[\mathrm{s}]}$, $\tilde{\varepsilon}_{\mu;\nu,k}$ differs from $\varepsilon_{\mu;\nu,k}$. We are thus led to equations having the form of the traditional PPP equations, but to solve the problem, the variance-covariance matrices of $\tilde{\varepsilon}_{\phi;\nu,k}$ and $\tilde{\varepsilon}_{p;\nu,k}$ are then to be properly taken into account.

4.4. Other approaches: similarities and differences

In its principle, our approach is similar to that defined in Ge *et al* (2005, 2006). Its implementation, which benefits from Property 2, is however much simpler. Furthermore, as the number of independent double differences is at most equal to the number of closure delays (see Remark 2.4), it is not generally optimal to work with a maximum set of independent double differences; see Figs. 3 & 4, and de Jonge 1998. Moreover, in our approach, Eq. (31) is then read as

$$\check{\Phi}_{\nu,k}^0 = \mathrm{A}_{\phi;\nu,k} u_k + \mathrm{B}_k v_{\mathrm{b}} + \tilde{\beta}_{\phi;\nu,k} + \varepsilon_{\phi;\nu,k} \quad (41)$$

where

$$\check{\Phi}_{\nu,k}^0 := \Phi_{\nu,k}^0 - \lambda_\nu N_\nu^{[\mathrm{cd}]} \quad (42)$$

The CD ambiguity constraints are thus imposed in algebraic manner. The choice of the ionospheric variables is also based on Property 2; see Eqs. (25) to (29). Furthermore, the satellite-bias information to be broadcasted to the network user is not the same. At last but not the least, the carrier-phase ambiguities have not to be fixed, a problem which cannot be easily solved. Indeed, as shown below, when the CD ambiguities are fixed, or when a maximum set of independent DD ambiguities is fixed, the remaining float problem is not of full rank.

Let us first consider the case where the CD ambiguities are fixed. To show that the problem is not then of full rank, let us assume that the receiver ambiguities $N_\nu^{[\mathrm{r}]}(i)$ are also fixed, and that all the variables are known except the satellite clock biases

$$f_{\phi;k}^{[\mathrm{s}]}(j) := f_{\phi;k}^{(\mathrm{s})}(j) - f_{\phi;k}^{(\mathrm{s})}(1) \quad (43)$$

and the satellite ambiguities $N_\nu^{[\mathrm{s}]}(j)$ for $j \neq 1$. The phase equation (1) then yields an equation of the form

$$\Gamma_{\nu,k}(i, j) = -f_{\phi;k}^{[\mathrm{s}]}(j) + \lambda_\nu N_\nu^{[\mathrm{s}]}(j) + \varepsilon_{\phi;\nu,k}(i, j) \quad (44)$$
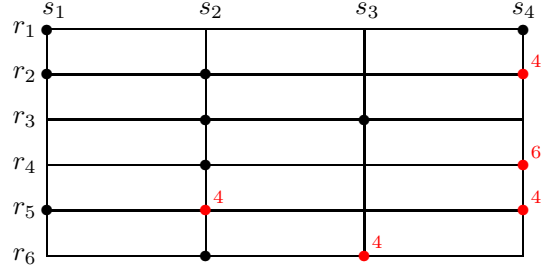

Figure 4: *Equivalent sets of CD ambiguities and independent DD ambiguities.* The scenario considered here corresponds to that of Fig. 3 in the DD approach: grid point $(1,3)$ was discarded. With regard to the selected spanning tree, we then have 4 loops of order 4, and one loop of order 6. The DD ambiguities of the CD function defined by the CD ambiguities (47) are the DD ambiguities of the maximum set of independent DD ambiguities (46). In other words, the maximum set of independent DD ambiguities (46) is equivalent to the set of CD ambiguities (47).

where $\Gamma_{\nu,k}$ is a known function. For any $\zeta(j) \in \mathbb{R}$, we then have

$$-f_{\phi;k}^{[\mathrm{s}]}(j) + \lambda_\nu N_\nu^{[\mathrm{s}]}(j)$$
$$= -[f_{\phi;k}^{[\mathrm{s}]}(j) + \zeta(j)] + \lambda_\nu \left[N_\nu^{[\mathrm{s}]}(j) + \frac{\zeta(j)}{\lambda_\nu} \right] \quad (45)$$

The solution of the corresponding float problem is therefore not unique: the problem is not of full rank. As a result, the satellite integer ambiguities $N_\nu^{[\mathrm{s}]}(j)$ cannot be easily obtained, hence the less ambitious approach proposed in this paper.

As expected, in the case where a maximum set of independent DD ambiguities is fixed, this analysis also holds. To clarify this point in an elementary manner, let us consider the scenario of Fig. 3 in which grid point $(1,3)$ is not taken into account; see Fig. 4. The following five DD ambiguities then form a maximum set of independent DD ambiguities (see, e.g., Saalfeld 1999):

$$\left|\begin{array}{l} N_\nu^{[\mathrm{dd}]}(1) := N_\nu(1,1) - N_\nu(1,4) + N_\nu(2,4) - N_\nu(2,1) \\ N_\nu^{[\mathrm{dd}]}(2) := N_\nu(1,1) - N_\nu(1,4) + N_\nu(5,4) - N_\nu(5,1) \\ N_\nu^{[\mathrm{dd}]}(3) := N_\nu(2,1) - N_\nu(2,2) + N_\nu(5,2) - N_\nu(5,1) \\ N_\nu^{[\mathrm{dd}]}(4) := N_\nu(3,2) - N_\nu(3,3) + N_\nu(6,3) - N_\nu(6,2) \\ N_\nu^{[\mathrm{dd}]}(5) := N_\nu(2,2) - N_\nu(2,4) + N_\nu(4,4) - N_\nu(4,2) \end{array}\right. \quad (46)$$

With regard to the selected spanning tree in Fig. 4, this set of DD ambiguities is equivalent to the following set of CD ambiguities:

$$\left|\begin{array}{l} N_\nu^{[\mathrm{cd}]}(2,4) = N_\nu^{[\mathrm{dd}]}(1) \\ N_\nu^{[\mathrm{cd}]}(4,4) = N_\nu^{[\mathrm{dd}]}(1) + N_\nu^{[\mathrm{dd}]}(5) \\ N_\nu^{[\mathrm{cd}]}(5,2) = N_\nu^{[\mathrm{dd}]}(3) \\ N_\nu^{[\mathrm{cd}]}(5,4) = N_\nu^{[\mathrm{dd}]}(2) \\ N_\nu^{[\mathrm{cd}]}(6,3) = N_\nu^{[\mathrm{dd}]}(4) \end{array}\right. \quad (47)$$

Lannes et al: Pseudo-clock biases for precise point positioning. The algebraic approach

75

We are thus brought back to the previous CD analysis. A general study of the DD-CD relationship is to be found in Lannes and Teunissen 2010/11.

5.   Receiver and Satellite Pseudo-Clock Biases

In Sect. 5.1, we first define the GNSS-delay spaces of type $\psi = (\phi; \nu)$ or $(p; \nu)$. In this framework, the pseudo-clock biases are obtained via the optimization principle presented in Sect. 5.2. To illustrate our analysis in a concrete manner, we finally consider an important special case (Sect. 5.3).

5.1. Edge-delay space of type ψ

As already specified (see Sect. 2.1), a function ϑ taking its values on G can be regarded as a vector of the edge-delay space E. In this Euclidean space, the norm of ϑ is defined by the relation

$$\|\vartheta\|^2 = \sum_{(i,j)\in G} |\vartheta(i,j)|^2 \tag{48}$$

We now adopt the notation according which

$$\Psi_{\psi,k} := \begin{cases} \Phi_{\nu,k} & \text{if } \psi = (\phi; \nu) \\ P_{\nu,k} & \text{if } \psi = (p; \nu) \end{cases} \tag{49}$$

The variance-covariance matrix of $\Psi_{\psi,k}$ is then denoted by $[V_{\psi,k}]$. Let us now consider a function ϑ of type ψ, for example a phase observational residual. At epoch k, the quadratic size of such a function is defined by the relation

$$\begin{aligned} \|\vartheta\|_{\psi,k}^2 &:= \quad [\vartheta]^{\mathrm{T}}[V_{\psi,k}]^{-1}[\vartheta] \\ &\equiv \quad (\vartheta \cdot V_{\psi,k}^{-1}\vartheta) \end{aligned} \tag{50}$$

Here, $[\vartheta]$, is the column matrix whose entries are the components of ϑ on G; $(\,\cdot\,)$ is the inner product of the Euclidean space E. The space of functions ϑ with inner product

$$\langle \vartheta' \mid \vartheta \rangle_{\psi,k} := (\vartheta' \cdot V_{\psi,k}^{-1}\vartheta) \tag{51}$$

is denoted by $E_{\psi,k}$. This space is referred to as the 'edge-delay space' of type ψ at epoch k.

Let us now introduce the following Cholesky factorization of the inverse of $[V_{\psi,k}]$:

$$[V_{\psi,k}]^{-1} = [U_{\psi,k}]^{\mathrm{T}}[U_{\psi,k}] \tag{52}$$

In this equation, $[U_{\psi,k}]$ is an invertible upper-triangular matrix. From Eq. (50), we then have (see Eq. (48))

$$\|\vartheta\|_{\psi,k} = \|\vartheta_{\psi,k}^{\mathrm{E}}\| \tag{53}$$

where

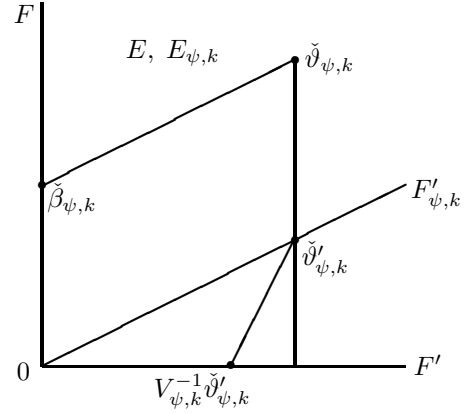$$\vartheta_{\psi,k}^{\mathrm{E}} := U_{\psi,k}\,\vartheta \tag{54}$$

Figure 5: *Pseudo-clock delay.* In this geometrical illustration, $E_{\psi,k}$ is the edge-delay space of type ψ at epoch k; F is the bias-delay space; $F'_{\psi,k}$ is the orthogonal complement of F in $E_{\psi,k}$, whereas F' is the orthogonal complement of F in the Euclidean space E. The functions lying in F' satisfy the centralization property 3. The pseudo-clock delay $\check{\beta}_{\psi,k}$ is the orthogonal projection of $\check{\vartheta}_{\psi,k}$ on F in $E_{\psi,k}$, whereas $\check{\vartheta}'_{\psi,k}$ is the orthogonal projection of $\check{\vartheta}_{\psi,k}$ on $F'_{\psi,k}$: $\check{\vartheta}'_{\psi,k} = \check{\vartheta}_{\psi,k} - \check{\beta}_{\psi,k}$. According to Property 4, $V_{\psi,k}^{-1}\check{\vartheta}'_{\psi,k}$ lies in F'. In the special case where the variance-covariance matrix of $\Psi_{\psi,k}$ is proportional to the identity, $F'_{\psi,k}$ coincides with F'.

5.2. Optimization principle

In the context previously defined, Eqs. (41) and (32) are of the form

$$\check{\Psi}_{\psi,k}^0 = \mathrm{A}_{\psi,k}u_k + \mathrm{B}_k v_{\mathrm{b}} + \tilde{\beta}_{\psi,k} + \varepsilon_{\psi,k} \tag{55}$$

where (see Eq. (42))

$$\check{\Psi}_{\psi,k}^0 := \begin{cases} \check{\Phi}_{\nu,k}^0 & \text{if } \psi = (\phi; \nu) \\ P_{\nu,k}^0 & \text{if } \psi = (p; \nu) \end{cases} \tag{56}$$

Note that $\tilde{\beta}_{\psi,k}$ lies in F; see the context of Eq. (9). Let us then set

$$\check{\vartheta}_{\psi,\kappa} := \check{\Psi}_{\psi,\kappa}^0 - (\mathrm{A}_{\psi,\kappa}\check{u}_k + \mathrm{B}_k\check{v}_{\mathrm{b}}) \tag{57}$$

where $\check{u}_k$ and $\check{v}_{\mathrm{b}}$ are defined in Sect. 4.2. The optimal estimate of $\tilde{\beta}_{\psi,k}$, referred to as the 'pseudo-clock delay,' is therefore defined by the relation (see Eq. (55))

$$\check{\beta}_{\psi,k} := \underset{\beta \in F}{\mathrm{argmin}}\ \|\check{\vartheta}_{\psi,k} - \beta\|_{\psi,k}^2 \tag{58}$$

Clearly, $\check{\beta}_{\psi,k}(i,j) = \check{\delta}_{\psi,k}^{[\mathrm{r}]}(i) + \check{\delta}_{\psi,k}^{[\mathrm{s}]}(j)$; see Eq. (30).

As illustrated in Fig. 5, $\check{\beta}_{\psi,k}$ is the point of F closest to ϑ, the distance being that induced by the norm defined on $E_{\psi,k}$; $\check{\beta}_{\psi,k}$ is therefore the projection of $\check{\vartheta}_{\psi,k}$ on F in $E_{\psi,k}$. Denoting by F' the orthogonal complement

Lannes et al: Pseudo-clock biases for precise point positioning. The algebraic approach

76

of F in E, we then have the following properties (see Fig. 5, and Sect. 5.2 in Lannes and Gratton 2009).

Property 3. *The functions lying in F' satisfy the following 'centralization conditions:'*

$$\left|\begin{array}{l} \sum_{j\in\mathcal{L}_i} \vartheta(i,j) = 0 \quad \text{(for } i=1,\ldots,m) \\[2ex] \sum_{i\in\mathcal{C}_j} \vartheta(i,j) = 0 \quad \text{(for } j=2,\ldots,n) \end{array}\right.$$

Property 4. *The pseudo-clock delay $\check{\beta}_{\psi,k}$ is the function β of F for which $V_{\psi,k}^{-1}(\check{\vartheta}_{\psi,k} - \beta)$ lies in F'.*

5.3. Reference special case

To illustrate our analysis in a concrete manner, we now consider the important special case where the variance-covariance matrix of the observational data $\Psi_{\psi,k}$ is diagonal (see Liu 2002):

$$[V_{\psi,k}] = \sigma_\psi^2 \operatorname{diag}\big(\eta_k(i,j)\big) \qquad \text{(on } G) \qquad (59)$$

Here, σ_ψ^2 is a 'reference variance;' $\eta_k(i,j)$ is a nonnegative weight function.

For clarity, let us then set

$$\check{\vartheta}_{i,j} := \check{\vartheta}_{\psi,k}(i,j) \qquad\qquad\qquad (60)$$

$$\check{\delta}_{r,i} := \check{\delta}_{\psi,k}^{[r]}(i) \qquad \check{\delta}_{s,j} := \check{\delta}_{\psi,k}^{[s]}(j) \qquad (61)$$

and

$$\omega_{i,j} := \left\{\begin{array}{ll} \dfrac{1}{\eta_k(i,j)} & \text{on } G; \\[2ex] 0 & \text{otherwise} \end{array}\right. \qquad (62)$$

From Properties 4 and 3, we then have (see Eqs. (4), (5) and (30))

$$\left|\begin{array}{l} \sum_{j\in\mathcal{L}_i} \omega_{i,j}\big[\check{\vartheta}_{i,j} - \big(\check{\delta}_{r,i} + \check{\delta}_{s,j}\big)\big] = 0 \quad \text{(for } i=1,\ldots m) \\[2ex] \sum_{i\in\mathcal{C}_j} \omega_{i,j}\big[\check{\vartheta}_{i,j} - \big(\check{\delta}_{r,i} + \check{\delta}_{s,j}\big)\big] = 0 \quad \text{(for } j=2,\ldots n) \end{array}\right.$$

i.e.,

$$\left|\begin{array}{l} \sum_{j\in\mathcal{L}_i} \omega_{i,j}\big(\check{\delta}_{r,i} + \check{\delta}_{s,j}\big) = \sum_{j\in\mathcal{L}_i} \omega_{i,j}\check{\vartheta}_{i,j} \quad \text{(for } i=1,\ldots m) \\[2ex] \sum_{i\in\mathcal{C}_j} \omega_{i,j}\big(\check{\delta}_{r,i} + \check{\delta}_{s,j}\big) = \sum_{i\in\mathcal{C}_j} \omega_{i,j}\check{\vartheta}_{i,j} \quad \text{(for } j=2,\ldots n) \end{array}\right.$$

We are thus led to introduce the quantities

$$\left|\begin{array}{ll} \Omega_{r,i} := \sum_{j\in\mathcal{L}_i} \omega_{i,j} & \text{(for } i=1,\ldots m) \\[2ex] \Omega_{s,j} := \sum_{i\in\mathcal{C}_j} \omega_{i,j} & \text{(for } j=2,\ldots n) \end{array}\right.$$

and

$$\left|\begin{array}{ll} \check{\vartheta}_{r,i} := \sum_{j\in\mathcal{L}_i} \omega_{i,j}\check{\vartheta}_{i,j} & \text{(for } i=1,\ldots m) \\[2ex] \check{\vartheta}_{s,j} := \sum_{i\in\mathcal{C}_j} \omega_{i,j}\check{\vartheta}_{i,j} & \text{(for } j=2,\ldots n) \end{array}\right.$$

The equations to be solved to determine $\check{\delta}_{r,i}$ and $\check{\delta}_{s,j}$ can then be written in the form

$$\left|\begin{array}{l} \Omega_{r,i}\,\check{\delta}_{r,i} + \sum_{j=2}^n \Omega_{i,j}\,\check{\delta}_{s,j} = \check{\vartheta}_{r,i} \quad \text{(for } i=1,\ldots m) \\[2ex] \sum_{i=1}^m \Omega_{i,j}\,\check{\delta}_{r,i} + \Omega_{s,j}\,\check{\delta}_{s,j} = \check{\vartheta}_{s,j} \quad \text{(for } j=2,\ldots n) \end{array}\right.$$

i.e., in matrix terms,

$$\left|\begin{array}{l} [\Omega_r]\,[\check{\delta}_r] + [\Omega][\check{\delta}_s] = [\check{\vartheta}_r] \\[1ex] [\Omega]^T[\check{\delta}_r] + [\Omega_s][\check{\delta}_s] = [\check{\vartheta}_s] \end{array}\right. \qquad (63)$$

Note that $[\Omega_r]$ is an $m \times m$ diagonal matrix, while $[\Omega_s]$ is an $(n-1)\times(n-1)$ diagonal matrix; $[\Omega]$ has m lines and $n-1$ columns. The inverses of $[\Omega_r]$ and $[\Omega_s]$ are trivial. As clarified below, Eq. (63) can be solved by computing the inverse of a matrix with size $(n-1)\times(n-1)$.

From the first equation (63), we have

$$[\check{\delta}_r] = [\Omega_r]^{-1}\big([\check{\vartheta}_r] - [\Omega][\check{\delta}_s]\big) \qquad (64)$$

hence, from the second,

$$[\Omega]^T[\Omega_r]^{-1}\big([\check{\vartheta}_r] - [\Omega][\check{\delta}_s]\big) + [\Omega_s][\check{\delta}_s] = [\check{\vartheta}_s]$$

i.e.,

$$[\Omega_{sr}][\check{\delta}_s] = [\check{\vartheta}_s] - [\Omega]^T[\Omega_r]^{-1}[\check{\vartheta}_r]$$

where $[\Omega_{sr}]$ is the following $(n-1)\times(n-1)$ matrix:

$$[\Omega_{sr}] := [\Omega_s] - [\Omega]^T[\Omega_r]^{-1}[\Omega] \qquad (65)$$

It then follows that

$$[\check{\delta}_s] = [\Omega_{sr}]^{-1}\big([\check{\vartheta}_s] - [\Omega]^T[\Omega_r]^{-1}[\check{\vartheta}_r]\big) \qquad (66)$$

If need be, Eq. (64) then yields $[\check{\delta}_r]$.

6.   Concluding Comments

This paper, which appeals to elementary notions of algebraic graph theory, completes the study presented in Lannes and Gratton 2009. Once the CD ambiguities have been fixed, particular satellite biases can be estimated and broadcasted to the network users for their precise point positioning. For example, in the case of large networks, each of these biases includes three (or four) terms: a satellite-clock term, a satellite time-group term, a satellite ionospheric term, and (for the phase)

Lannes et al: Pseudo-clock biases for precise point positioning. The algebraic approach

77

a satellite integer ambiguity multiplied by the corresponding wavelength; see Eqs. (26), (27), (24), (16), (17) and (18). The form of the PPP equations to be solved by the network user is then the same as that of the traditional PPP equations; see Eqs. (39) and (40).

As soon as the CD ambiguities are fixed and validated, estimates of these float biases can be obtained. The corresponding operation simply amounts to solving a linear system whose size is equal to the number of satellites other than the reference satellite; see Eqs. (66) and (65). The main result of this paper is that no other ambiguity is then to be fixed, hence a better efficiency. In particular, in this approach, it is not necessary to fix the carrier-phase ambiguities, a problem which cannot be easily solved; see Sect. 4.4.

The principle of our strategy differs from that of Ge *et al* (2005, 2006). Its implementation, which is based on Property 2, is much simpler. In particular, the CD ambiguity constraints are imposed in algebraic manner; see Eqs. (41) and (42). The choice of the ionospheric variables is also based on Property 2; see Eqs. (25) to (29). Furthermore, the satellite-bias information to be broadcasted to the network user is not the same. At last but not the least, as already emphasized, this information is obtained without fixing the carrier-phase ambiguities.

Acknowledgements

References

Biggs N. (1996) *Algebraic graph theory*, 2nd edition Cambridge University Press, Cambridge.

Björck A. (1996) *Numerical methods for least-squares problems*, SIAM.

Feng Y. and Li B. (2008) *Three-carrier ambiguity resolution: generalized problems, models, methods and performance analysis using semi-generated triple frequency GPS data*. Proc. ION GNSS-2008. Savannah, Georgia USA: 2831-2840.

Ge M., Gendt G., Dick G. and Zhang F.P. (2005) *Improving carrier-phase ambiguity resolution in global GPS networks solutions*. J. Geod. 79: 103–110.

Ge M., Gendt G., Dick G., Zhang F.P. and Rothacher (2006) *A new data processing strategy for huge GNSS global networks*. J. Geod. 80: 199–203.

Jonge P.J. de (1998) *A processing strategy for the application of the GPS in networks*. PhD dissertation. Netherlands Geodetic Commission, 46.

Lannes A. and Gratton S. (2008) *QR implementation of GNSS centralized approaches*. J. GPS. 7: 133–147.

Lannes A. and Gratton S. (2009) *GNSS networks in algebraic graph theory*. J. GPS. 8: 53–75.

Lannes A. and Teunissen P.J.G. (2010/11) *GNSS algebraic structures*. To appear in J. Geod.

Liu X. (2002) *A comparison of stochastic models for GPS single differential kinematic positioning*. Proc. ION GPS-2002. Portland, Oregon USA: 1830-1841.

Saalfeld A. (1999) *Generating basis sets of double differences*. J. Geod. 73: 291–297.

Teunissen P.J.G. (1984) *Generalized inverses, adjustment, the datum problem and S-transformations.* Lecture notes International School of Geodesy, Erice, Italy, April 25-May 10.

Teunissen P.J.G. and Kleusberg A. (1998) *GPS for Geodesy*, 2nd edition, Springer Verlag.

Biography

Dr. André Lannes (Andre.Lannes@lss.supelec.fr) was born in France in 1946. Director of Research at the CNRS (Centre National de la Recherche Scientifique), he has published about one hundred papers in solid state physics, electron microscopy, optics, applied mathematics, and image processing in astronomy & geophysics. He also worked as a project leader at the CERFACS: "Centre Européen de Recherche et de Formation Avancé en Calcul Scientifique" (European Centre for Research and Advanced Training in Scientific Computation). His main researches were devoted to image reconstruction in aperture synthesis with particular reference to phase-closure imaging (radio imaging, optical interferometry). In a Note published by the French 'Académie des Sciences' in 2001, he showed that the integer-ambiguity problems of phase-closure imaging share a common feature with those of differential GPS. His GNSS contributions derive from this global vision.